Hybrid Renewable Energy System with High Gain Modified Z-Source Boost Converter for Grid-Tied Applications

Sathish Ch.[1], Chidambaram I.A.,[1] Manikandan M.[2]

[1]Annamalai University, Tamilnadu, India
[2]Jyothishmathi Institute of Technology and Science, Telangana, India

Abstract. In a hybrid renewable system, a conventional boost converter produces more losses at the time of the energy conversion process due to this, the performance of the hybrid system is reduced total harmonic distortion is increased, and the hybrid microgrid outcome is reduced. The main objective of the work enhancing the low DC voltage produced by the PV panel, a high gain Boost converter is utilized. The objectives of the work were achieved by a High Gain Modified Z-source Boost converter along with Modified Particle Swarm Optimized- Proportional Integral (MPSO-PI) controller employed in the energy conversion stage at Grid. It reduced power conversion stages and decreases the losses compared to existing Hybrid Grid-connected systems. A new 13-bus system is developed in this work for regulating the output voltage in distribution networks. The significance of our work lies in the design of an efficient microgrid system for grid-tied applications. High Gain Modified Z-source Boost converter along with Modified Particle Swarm Optimized- Proportional Integral (MPSO-PI) controller is employed to boost the voltage obtained from the PV system. A battery converter along with a bi-directional battery is connected to the DC link, to store energy generated by Hybrid Renewable Energy System (HRES) in excess amounts. The obtained DC link voltage is transferred to Three Phase VSI for the conversion of DC to AC voltage. Effective harmonic reduction is attained with the aid of an LC filter coupled to Three Phase grid, and the PI controller connected to Voltage Source Inverter(VSI) supports achieving effective grid synchronization. The proposed work was tested with 13 bus system through MATLAB Simulink.

Keywords: hybrid renewable energy system, photovoltaic system, total harmonic distortion, 13 bus system, switched Z-source boost converter.

DOI: https://doi.org/10.52254/1857-0070.2023.1-57.04

UDC: 621.311

Sistemul energetic hibrid cu surse regenerabile de energie și cu convertizor de tip Z modificat pentru conectare directă la rețea

Sathiș Ch.[1], Cidambaram I.A.,[1] Manikandan M. [2]

[1] Universitatea Annamalai, India, [2]Jyothishmathi Institute de Technologia și Știința, India

Rezumat. În sistemul energetic hibrid cu SER, convertorul boost convențional generează mai multe pierderi în timpul procesului de conversie, determinând scăderea performanței sistemului hibrid, creșterea distorsiunii armonice totale și scăderea eficienței microrețelei hibride. Scopul principal al lucrării este de a ridica tensiunea DC scăzută generată de panoul fotovoltaic folosind un boost convertor cu coeficientul de amplificare înaltă. Obiectivele lucrării au fost atinse utilizând un boost convertor cu coeficientul de amplificare înaltă de tip Z modificat împreună cu un controler PI optimizat prin metoda roiului de particule și utilizat în treaptă de conversie energiei în rețea. Astfel încât a micșorat numărul etapelor de conversie a energiei și a micșorat pierderile în comparație cu sistemele existente conectate la rețea hibridă. În această lucrare, am elaborat un nou sistem cu 13 șine pentru reglarea tensiunii de ieșire în rețelele de distribuție. Semnificația lucrării constă în elaborarea unui sistem de microrețea eficient pentru aplicații în rețele. Convertorul boost co coieficient de amplificare înalt și cu Z- sursă modificat, împreună cu un controler PI modificat, optimizat prin metoda roiului de particole este folosit pentru creșterea tensiunii din sistemul fotovoltaic. Convertorul bateriei, împreună cu bateria bidirecțională, este conectat la legătura DC pentru a stoca surplusul de energie generat de sistemul hibrid de energie regenerabilă. Tensiunea rezultată a circuitului de curent continuu este transferată la un convertor trifazat DC/AC. Suprimarea eficientă a armonicilor este realizată cu un filtru LC conectat la rețeaua trifazată, iar un controler PI conectat la invertorul sursei de tensiune (VSI) asigură o sincronizare eficientă a rețelei.

***Cuvinte-cheie*:** sistem hibrid cu surse de energie regenerabilă, sistem fotovoltaic, distorsiune armonică totală, sistem cu 13 șine, convertizor de amplificare cu comutare Z-sursa.

Гибридная энергосистема с возобновляемыми источниками энергии и с модифицированным повышающим преобразователем Z-типа для непосредственной связи с сетью

Чиндам С.[1], Чидамбарам И.А.[1], Маникандан М.[2]
[1]Университет Аннамалай, Индия, [2]Институт технологии и наук Джотишмати, Телангана, Индия

Аннотация. В гибридной энергосистеме на ВИЭ обычный повышающий преобразователь создает больше потерь во время процесса преобразования из-за чего производительность гибридной системы снижается, общие гармонические искажения увеличиваются, а эффективность гибридной микросети снижается. Основной целью работы является повышение низкого напряжения постоянного тока, создаваемого фотоэлектрической панелью, с использованием повышающего преобразователя с высоким коэффициентом усиления. Цели работы были достигнуты с помощью повышающего преобразователя с модифицированным Z-источником и с высоким коэффициентом усиления вместе с модифицированным ПИ-регулятором, оптимизированным с помощью метода роя частиц, используемым в ступени преобразования энергии в сети. Это уменьшило число этапов преобразования энергии и уменьшило потери по сравнению с существующими системами, подключенными к гибридной сети. В данной работе разработана новая 13-шинная система для регулирования выходного напряжения в распределительных сетях. Значение работы заключается в разработке эффективной микросетевой системы для сетевых приложений. Повышающий преобразователь с модифицированным Z-источником с высоким коэффициентом усиления вместе с модифицированным пропорционально-интегральным контроллером, оптимизированным методом роя частиц используется для повышения напряжения, получаемого от фотоэлектрической системы. Аккумуляторный преобразователь вместе с двунаправленной батареей подключен к звену постоянного тока для хранения избыточной энергии, вырабатываемой гибридной системой возобновляемых источников энергии. Полученное напряжение звена постоянного тока передается на трехфазный преобразователь постоянного напряжения в переменное. Эффективное подавление гармоник достигается с помощью LC-фильтра, подключенного к трехфазной сети, а ПИ-регулятор, подключенный к инвертору источника напряжения (VSI), обеспечивает эффективную синхронизацию сети. Предлагаемая работа была протестирована с 13-шинной системой с помощью MATLAB Simulink.

Ключевые слова: гибридная система с возобновляемыми источниками энергии, фотоэлектрическая система, полное гармоническое искажение, система с 13 шинами, повышающий преобразователь с переключаемым Z-источником.

INTRODUCTION

Energy supply and utilization challenges are associated with environmental issues like air pollution, acid rain, depletion of the ozone layer, deforestation, and radioactive emissions in addition to global warming [1]. Potential countermeasures include reducing the usage of fossil fuels, increasing the availability of ecologically acceptable energy sources, and improving energy efficiency to conserve energy [2]. To combat an energy problem and environmental degradation, it is crucial to produce RES. Energy Storage Systems (ESS) offers flexibility to lessen the effects of RE access to the grid because RE sources exhibit exceptional features of variable and uncertainty [3-5]. Solar and wind energy are the two most promising RES for producing electricity with the potential to make a sizable contribution to the world's electrical energy needs. Both of these resources are nearly limitless, free, and emit no harmful by-products or greenhouse gases [6]. However, there is a certain amount of unpredictability with solar and wind energy because they are weather-dependent sources. While the generation of solar energy is generally predictable, that of wind energy is sporadic, unreliable, and very unpredictable [7]. In this proposed work, hybrid power generation like Solar Photovoltaic [8] and WECS [9] has outperformed all other renewable energy sources due to a number of factors, including its availability in nature, environmental friendliness, minimal maintenance costs, and dependability. From an environmental standpoint, the primary goal of the proposed study is to emphasize on green energy by reducing the use of energy derived from fossil fuels for the distribution system. Typically, DC-DC converters are employed to regulate power generation and maximize electricity in varying climatic and environmental circumstances [10, 11]. In applications of a photovoltaic system, Boost converters [12] are frequently employed for DC-DC conversion, however, only step-up voltage ratios are feasible. The typical Buck-Boost converter [13], converts voltage in both step-up and step-down directions, but due to its interrupted input current, it cannot operate at its best without significant decoupling capacitors. Although Cuk [14] converter is capable of

stepping voltage up or down it seems to have constant input currents. The enormous input power ripples still limit the performance of the photovoltaic system under variable power points. The benefits of DC-DC Z-source [15] converters over traditional boost converters make them a great option for many applications involving renewable energies. However, since numerous discrete DC-DC converters must be employed, this is unworkable. To solve this problem, a Switched Z-Source driven DC-DC Boost converter is built, which uses fewer switches and is more efficient, and reduces power losses. Efficient control techniques are necessary for a converter, in order to attain reduced settling time, steady state error, peak overshoot and mitigate harmonics. In the proposed work, PI controller [16] is employed, which is a simple conventional control approach to control DC voltages. Distributed generation (DG) is a crucial component of contemporary power networks, which also include energy storage technologies, RES, and load types like electric vehicles, etc. [17]. The placement of the DGs ensures that they complement one another and maintain the microgrid's seamless operation. To assure improved operation of the microgrid in a grid-connected system, the control schemes within a module are created [18, 19]. In order to thoroughly investigate power quality disturbances and operating issues connected to the integration of RES into a balanced distribution network, this paper makes use of a standard IEEE 13-bus power system [20]. A z-source boost converter and An IEEE 13 bus system are employed in this architecture to obtain an equal amount of real and active power to the system by eliminating losses. This has multiple advantages as a lesser count of switches, high power processing capability, and high-reliability result in a reduction of the overall cost. Besides, the prime advantage of this topology is achieving high voltage gain for a low-duty ratio. These problems have not been previously considered in the literature and they are the subject of study in this article. The novelty of the work consists in the fact, that the non-linear voltage obtained from the PV system is improved with the utilization of a High Gain Modified Z-source boost converter, which provides isolation by stepping up the voltage. For efficient control of the converter, (MPSO-PI) controller is employed, which provides the optimal result with its simple design. When compared to other conventional controllers, the proposed control offers reduced oscillations with a better dynamic response. Similarly, the DFIG-based WECS associated with the proposed work generates AC voltage. In order to provide supply for the DC bus, the PWM rectifier coupled to the WECS converts the AC voltage to DC. The generated DC supply from both sources is transferred to the DC link. The battery converter combined with the battery system collects the excess energy produced by the RES for later usage. The 3Φ VSI provided converts DC voltage to AC, from which the voltage is supplied to LC filter for harmonics mitigation and supplied effectively to the grid. An IEEE 13 bus system is employed in this architecture to obtain an equal amount of real and active power to the system by eliminating losses. The performance of the hybrid approach for the distribution system is validated using MATLAB simulation and improved results are obtained.

OBJECT, SUBJECT, AND METHODS FOR RESEARCH

The main objective of this work is to design and develop a Hybrid Renewable energy model based on solar photovoltaic (PV) systems integrated with Wind Energy Conversion Systems (WECS) to generate and provide stable and maximum power during different electrical behavior like voltage sags, dips, harmonics, etc.

In the proposed work as shown in Figure 1, an efficient IEEE 13 bus distribution system is demonstrated for equal distribution of electricity to more supplies. HRES consisting of solar PV and WECS is proposed in this research for generating electricity by natural means.

However, the intermittent nature affects the system’s performance. In order to enhance the voltage obtained from the PV system, a converter approach is necessary. Usually, a DC-DC converter is employed to boost the voltage generated by the PV system. In this proposed work High Gain Modified Z-source Boost converter is implemented, which is an advanced form of the boost converter. The non-linear output from the PV is stabilized using an MPSO- PI controller to Switch the Z-source Boost converter. Similarly, DFIG-WECS is the other RES for generating energy, which produces AC voltage.

The acquired AC voltage is converted into DC with the aid of a PWM rectifier.

A bidirectional battery along with a converter is placed in the DC link to acquire the excess energy generated and for utilization during the intermittent. The interfacing of the battery to the microgrid is accomplished using a battery

converter and the SOC of the battery is managed using a PI controller.

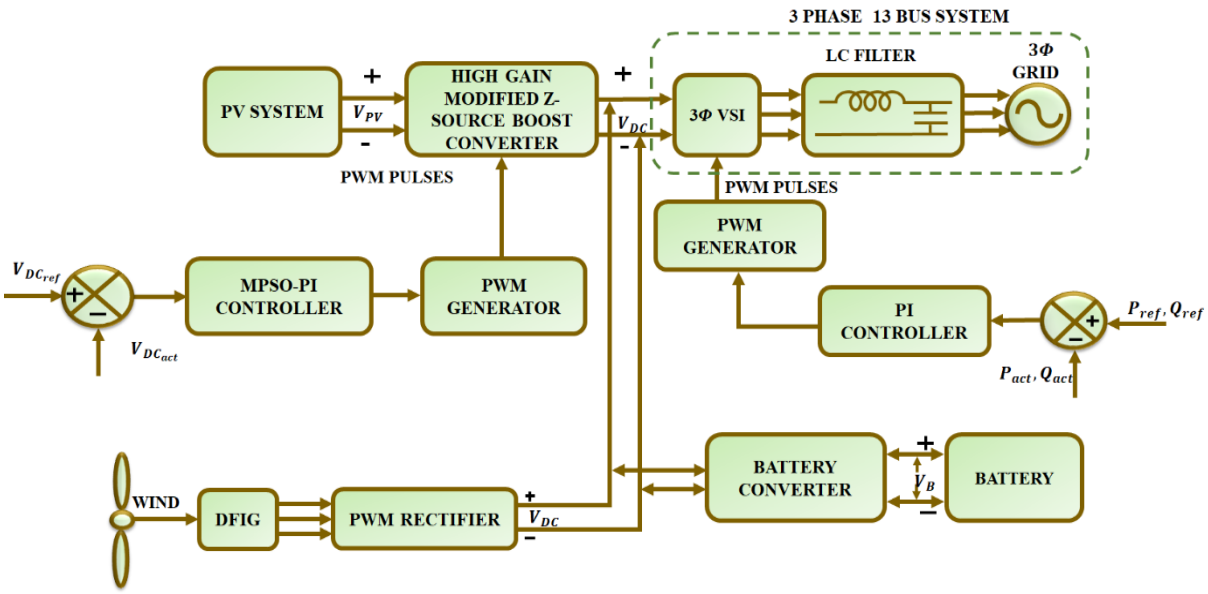

Fig. 1. Block diagram of proposed system.

Effective grid synchronization is also achieved by the control of 3ϕ VSI using the PI controller. The 3ϕ VSI connection to the grid via the LC filter results in effective harmonic mitigation. The 3ϕ IEEE 13 bus system provided in the proposed work reduces the unbalanced distribution and provides an equal power supply to different loads.

ANALYSIS OF THE MODEL AND THE METHODOLOGY OF ITS RESEARCH

A. PV Modelling

A PV system is made up of cells arranged in an array that is either stationary or moved by motors in order to monitor the sun and maximize the amount of power produced.

In addition to their high initial cost, one of the drawbacks of PV systems is that they require a lot of room to generate enough power.

PV systems were initially utilized for massive corporations with extensive networks, but they now it is used for household and commercial uses.

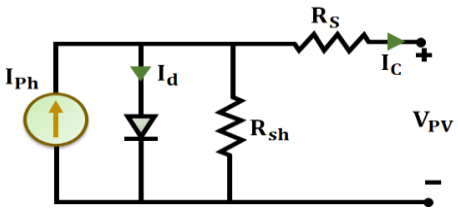

Fig. 2. Equivalent circuit of solar PV system.

By applying Kirchhoff's current law,

$$I_{PV} = I_{Ph} - I_d - I_P \tag{1}$$

$$\text{Here, } I_d = I_o\left[\exp\left(\frac{V_{PV} + I_{PV}R_S}{nv}\right) - 1\right] \tag{2}$$

$$I_p = \left(\frac{V_{PV} + I_{PV}R_S}{R_P}\right) \tag{3}$$

$$I_{PV} = I_{ph} - I_o\left[\exp\left(\frac{V_{PV} + I_{PV}R_S}{nv}\right) - 1\right] - \frac{V_{PV} + I_{PV}R_S}{R_P} \tag{4}$$

$$\text{Here, } V_{OC} = \frac{akT}{q} Log_n\left(\frac{I_{Ph}}{I_d} + 1\right) \tag{5}$$

The PV panel's open circuit voltage is,

$$V_{OC} = \frac{akT}{q} Log_n\left(\frac{I_{Ph}}{I_d} + 1\right) \tag{6}$$

Here, I_{PV} specifies the PV output current that flows through the series resistance R_S, V_{PV} specifies the PV output voltage I_{pb} specifies the photogenerated current, I_d specifies the diode saturation current, I_o specifies reverse saturation current, I_P specifies the current that flows through the shunt resistance R_P, n stands for number of series connected solar PV cells, v represents the junction thermal voltage, a stands for diode ideality constant, q represents the electron charge, whch has a value of, k denotes the Boltzmann

constant $(1.381 \cdot 10^{-23} J/K)$ and T stands for temperature of PN junction.

B. MPSO-PI Controller Technique

PI controller is one of the most often utilized controllers. There are two tuning parameters for PI controllers.The proportional section and integral section make up both of its components. Here, deviations in steady-state error are caused by the proportional part, simultaneously the integral part removes the steady-state error. The mismatch between a measured process parameter and the set reference point is used by a PI controller to determine an error value.

The output $u(t)$ specifies the PI controller at the time domain and is calculated as,

$$u(t) = k_p e(t) + \mathrm{k}_1 \int e(t)dt \tag{7}$$

Here, the error is denoted as $e(t)$, Proportional gain as k_p and k_1 specifies the integral gain factor evaluated from,

$$k_1 = \frac{k_p}{T_i} \tag{8}$$

Here, reset time is represented as T_i. Substituting Equation (8) in (7) the corresponding expression becomes,

$$u(t) = k_p e(t) + \frac{k_p}{T_i} \int e(t)dt \tag{9}$$

MPSO Algorithm

To create an initial population of swarms, where each member is referred to as a particle, the PSO algorithm provides a collection of stochastic solutions to the objective function. The population size of a swarm is defined as the total number of particles it contains. Each particle navigates the problem's solution space by following the ideal particle in the preceding batch along its own optimal pathways, much like a bird hunting for food. Every particle has the ability to change its position as determined by Equation (11) and velocity Equation (10). Earlier velocity and previous position for one's own personal best, and the current position for one's own global best all serve as indicators of the shift in velocity.
Particle velocity and position at the time $t+1$ is expressed by

$$V_{in}^{(t+1)} = \omega * V_{in}^{(t)} + C_1 * r_1 * \left(P_{in} - X_{in}^{(t)}\right) + \ldots \\ \ldots C_2 * r_2 * (G_{in} - X_{in}^{(t)}) \tag{10}$$

$$X_{in}^{(t+1)} = X_{in}^{(t)} + V_{in}^{(t+1)} \tag{11}$$

From the expression above, inertia at range 0-1 is given by w, acceleration constants as C_1 and C_2 random numbers as r_1 and r_2 ranging from 0 to 1. The fitness function acquired by the objective function, decides which position is superior in search space, and is applied to every new position. To increase computing efficiency, the particle velocity formula has been modified in proposed approach. C_1 and C_2 are constant variables in traditional PSO method, and they don't vary over time. In the modified PSO method, C_1 falls off and C_2 rises exponentially over time. Figure 3 illustrated the MPSO optimized PI controller flowchart. The time dependent effect of C_1 and C_2 are as follows: -

- With time, a particle's next position becomes less dependent on its best previous position.
- With time, particles' next positions become more and more dependent on global best position.
- The primary advantage of PSO is its ability to produce random particles, however after some time, when warm has encountered several alternative solutions, one of them will eventually emerge as the best option available. After this point, the swarm should only search in vicinity of best solution because it is quite likely that the optimal value for fitness function is present nearby.
- It is improbable that particles dispersed across the whole solution space will perform better than particles focused around a more compact subspace that contains the solution.In a very short period of time, the entire swarm gathers around single global best point and continues its search for global optimum in a very constrained subspace surrounding global best. Swarm optimization is improved and completed more quickly when it concentrates around a tiny subspace.

The expressions of Modified PSO velocity and position expressed as

$$V_{in}^{(t+1)} = \omega * V_{in}^{(t)} + C_1 * \left(P_{in} - X_{in}^{(t)}\right) + \ldots \quad (12)$$
$$\ldots C_2 * (G_{in} - X_{in}^{(t)})$$

$$X_{in}^{(t+1)} = X_{in}^{(t)} + V_{in}^{(t+1)} \quad (13)$$

The value of

$$\omega = 0.4, C_1 = e^{(-0.05t)}, C_2 = \frac{e^{(-0.05t)}}{\left(1 + 0.05e^{(-0.05t)}\right)}$$

Thus, effective parameter tuning of PI controller is achieved by means of MPSO technique.

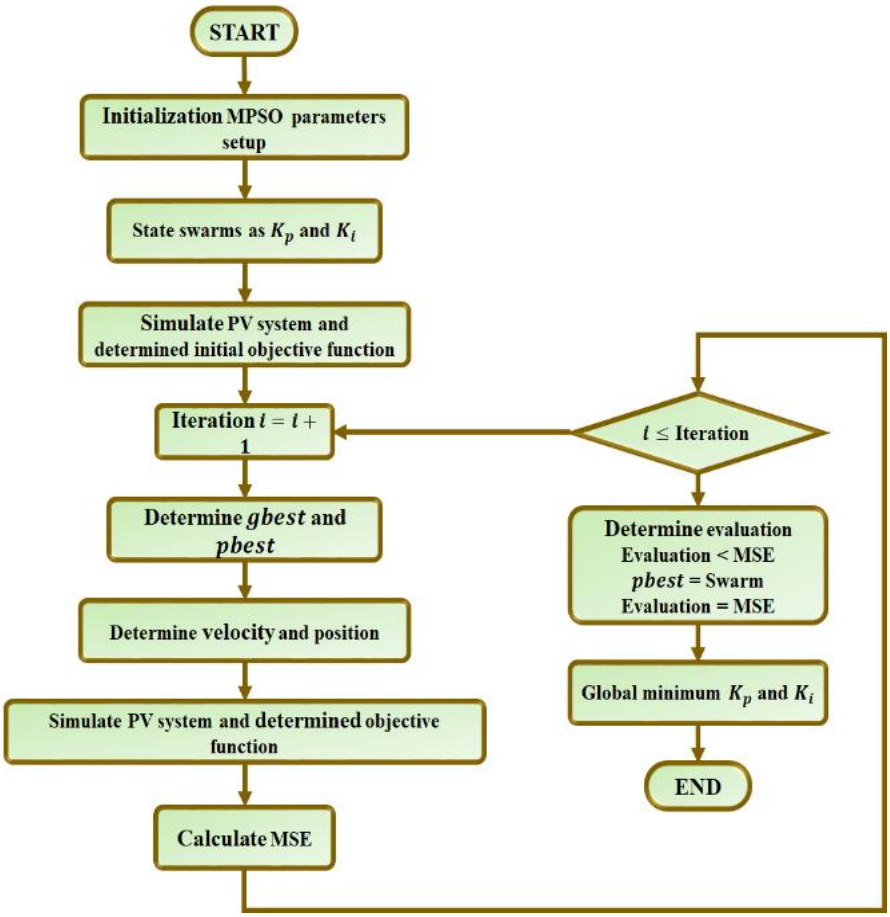

Fig. 3. MPSO-PI controller flow chart.

Grid Voltage Synchronization Using PI Controller

The PI controller minimizes the error, which is determined by comparing the actual output current of the inverter with the reference grid current. The proportional constant K_P and the integral constant K_I are the two different parameters that are involved in the calculation procedure of the controller. Here both proportional and integral operation takes place. In the case of proportional operation, the error e is multiplied with the gain K_P, whereas in the case of integral operation, the error e is integrated and then multiplied with gain K_I.

At the end of both operations, the steady-state error is totally minimized and the reference signal is generated in a short span of time. This controller is capable of working with both stationary reference frame $(\alpha\beta)$ and synchronous reference frame (dq). Here the PI controller is used in the dq reference frame for achieving effective grid voltage synchronization. The grid-connected inverter's output voltage in the synchronous (dq) frame is calculated using the inverter's mathematical model, as shown below.

$$\begin{bmatrix} u_d \\ u_q \end{bmatrix} = L\frac{d}{dt}\begin{bmatrix} i_d \\ i_q \end{bmatrix} + R\begin{bmatrix} i_d \\ i_q \end{bmatrix} + wL\begin{bmatrix} -i_q \\ i_d \end{bmatrix} + \begin{bmatrix} e_d \\ e_q \end{bmatrix} \quad (14)$$

Here, u_d and u_q are the Park transformation components of the inverter output, e_d and e_q are the park transformation components of the grid voltage. The resistance and inductance between the grid and the grid-connected inverter are denoted by the letters R and L, respectively. The angular frequency of the grid is specified as ω.

The current vector components indicated in the synchronous reference frame (dq) are compensated using two PI controllers One PI controller compares I_d and I_d^*, while the other compares I_d and I_d^*, and generate errors that are minimized to zero. The power factor and output power are regulated by varying the $q-$axis and $d-$currents.

PI controller-based BESS

The actual battery voltage V_{Bact} and the reference voltage V_{Bref} are compared to find the steady-state error e. This error is fed into the PI controller, which performs both proportional and integral control operations and generates the control signal u as shown below.

$$u = K_P e + K_1 \int e dt \tag{15}$$

The PWM generator generates PWM pulses based on the control signal, which is obtained from the PI controller. The resultant PWM pulses control the duty cycle of the battery converter in order to enable buck as well as boost mode of operation. The battery is charged during the buck mode of operation and discharged during the boost mode of operation.

C.Modelling of the DFIG system

The main components of a DFIG-based WECS are a Wind turbine, gearbox, wound-rotor induction machine, and a back-to-back converter. Wind speed has a direct connection with kinetic power, which is calculated as follows:

$$P_a = \frac{1}{2}\rho S C_P(\lambda, \beta) V^3 \tag{16}$$

Here, wind speed is specified as, air density as ρ with a value $1.225 kg/m^3$ area surrounded by turbine blades as S and power conversion efficiency Subsequently, the aerodynamic torque is expressed as,

$$T_a = \frac{p_a}{\Omega_t} = \frac{1}{2\Omega_t}\rho S C_P(\lambda, \beta) V^3 \tag{17}$$

Where turbine speed is represented as Ω_t .

A winding rotor asynchronous generator known as DFIG connects the grid directly to the stator and the rotor to the converter. The DFIG dynamic model utilized in this work is expressed in an arbitrary rotating frame for simplicity's sake. The voltage equations of the stator and rotor is expressed as,

$$\begin{cases} v_{ds} = R_S i_{ds} + \frac{d}{dt}\phi_{ds} - \omega_s \phi_{qs} \\ v_{qs} = R_S i_{qs} + \frac{d}{dt}\phi_{ds} - \omega_s \phi_{ds} \\ v_{dr} = R_r i_{dr} + \frac{d}{dt}\phi_{dr} - \omega_r \phi_{qr} \\ v_{qs} = R_r i_{qr} + \frac{d}{dt}\phi_{qr} - \omega_r \phi_{dr} \end{cases} \tag{18}$$

Here, the stator and rotor indices is denoteas S and r , synchronous reference components as d and q, the flux, current and voltage is specified as ϕ , v and i and resistance as R Similarly, the flux equations for stator and rotor are given by,

$$\begin{cases} \phi_{ds} = L_S i_{ds} + M i_{dr} \\ \phi_{qs} = L_S i_{qs} + M i_{qr} \\ \phi_{dr} = L_r i_{dr} + M i_{ds} \\ \phi_{qr} = L_r i_{qr} + M i_{qs} \end{cases} \tag{19}$$

This specifies inductance as L and mutual inductance as M .For a DFIG-WECS the mechanical equation is expressed as,

$$J\frac{d\Omega}{dt} = T_a - T_{em} - f\Omega \tag{20}$$

Here, total inertia of turbine is denoted as J , DFIG speed as Ω , Generator Electro-Magnetic (EM) torque as T_{em} and the damping coefficient as f The EM torque equation of DFIG is given by,

$$T_{em} = \rho\frac{M}{L_S}\left(\phi_{qs} i_{dr} - \phi_{ds} i_{qr}\right) \tag{21}$$

In which the number of pairs of poles in DFIG is represented as ρ .The corresponding active and reactive power at stator side is evaluated as,

$$\begin{cases} P_S = \frac{3}{2}(v_{ds} i_{ds} + v_{qs} i_{qs}) \\ Q_S = \frac{3}{2}(v_{qs} i_{ds} - v_{ds} i_{qs}) \end{cases} \tag{22}$$

D.High Gain Modified Z-Source Boost Converter

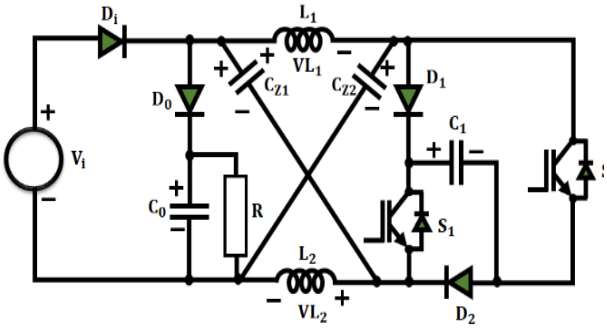

Fig. 4. Equivalent circuit topology of proposed converter.

An innovative High Gain Modified Z-source based boost converter is proposed, including strong step-up capability and minimal device voltage stress. The projected method provides input and output through a common ground that makes it more appropriate for specific applications. The topology of the proposed Converter constitutes of a switched capacitor cell, and a Z-source network. The identical drive signal concurrently controls switches S_1 and S_2. The suggested converter also includes a capacitor C_0, an output diode D_0 , and an input diode D_i .

Operating Modes of Proposed Converter :

This section compares and contrasts the Discontinuous Conduction Mode (DCM) Continuous Conduction Mode (CCM) operating philosophies. The following analysis makes the following presumptions. The capacitors are all of adequate sizes. As a result, the capacitors' voltage is conceived as constant for a switching period. The power equipment is perfect, and the parasitic components are ignored.Inductors L_1 and L_2 have same level of inductance due to the similarity of the topologie.

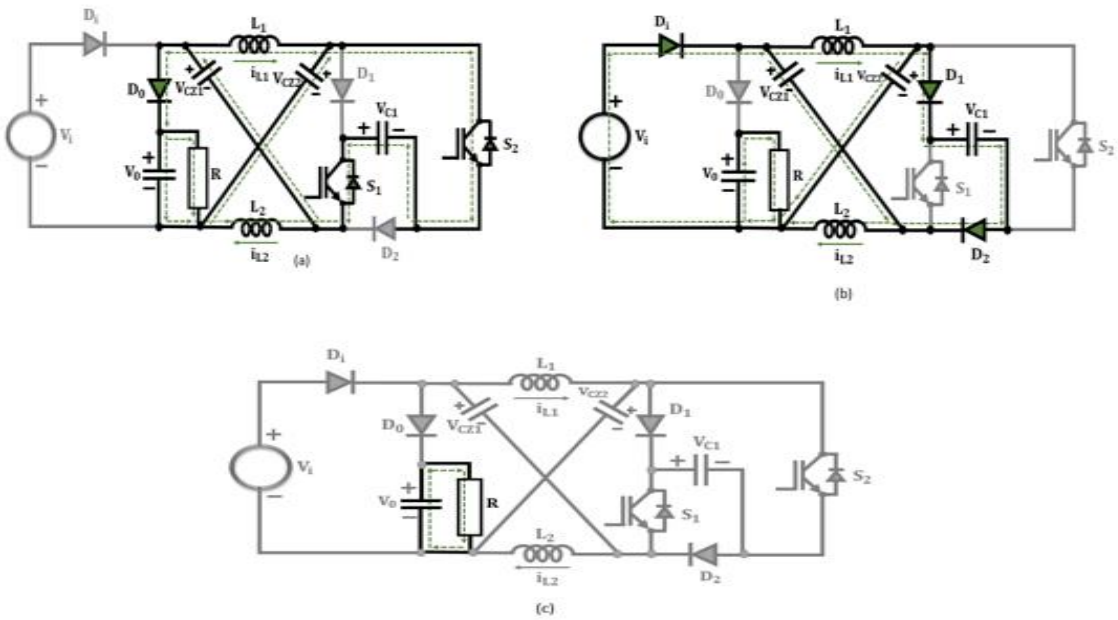

Fig. 5. Direction of current flow during (a) Mode1 at CCM &DCM, (b) Mode 2 at CCM &DCM and (c) Mode 3 DCM.

a)Operation at CCM

Mode 1:$[t_0 - t_1]$Switches S_1, S_2 and output diode D_0 are in ON state, and the diodes D_1, D_2 and D_i

are reversed biased using $V_0 - V_i$ and V_{C1}. The current flow is indicated in Figure 5(a).

The inductor L_1 is charged via capacitor C_{Z1} and C_1, while the other inductor L_2 is charged by C_{Z2} and C_2 capacitors. In the interim, C_{Z1}, C_{Z2} and C_1 linked in series to charge loads R and C_0. Equations (23) and (24) are acquired, in accordance with Kirchhoff Voltage Law (KVL).

$$\begin{cases} V_{L1} = V_{C1} + V_{CZ1} \\ V_{L2} = V_{C1} + V_{CZ2} \end{cases} \quad (23)$$

$$V_0 = V_{C1} + V_{CZ1} + V_{CZ2} \quad (24)$$

Mode2: $[t_1 - t_2]$ Diodes D_1, D_2 and D_i are turned ON and switches are turned OFF. The output diode D_0 is reversed biased by $V_0 - V_i$. The direction of the current flow is represented in Figure 5(b). The capacitor of the converter V_{CZ1} is charged by V_i and V_{CZ2} using V_i and L_1. The capacitor C_1 is charged additionally, by inductors L_1, L_2 and V_i. C_0 Is responsible for sustaining the output voltage. These connections are made, according to KVL.

$$\begin{cases} V_{L1} = V_i - V_{CZ2} \\ V_{L2} = V_i - V_{CZ1} \end{cases} \quad (25)$$

$$V_{C1} = V_{CZ1} + V_{CZ2} - V_i \quad (26)$$

b)Operation at DCM

In DCM mode 3 Operating Modes are there

Mode 1 : [t_0 - t_1] The circuit topology is same as that of in CCM and Equations (23) and (24) are still applicable at this stage. Considering $L_1 = L_2 = L$, the fluctuation of inductor current throughout this time period can be estimated as follows,

$$\left\{ \Delta i_{L1} = \frac{(V_{CZ1} + V_{C1})}{L} DT_S \right. \quad (27)$$

$$\left\{ \Delta i_{L2} = \frac{(V_{CZ2} + V_{C2})}{L} DT_S \right. \quad (28)$$

Mode 2: [$t_1 - t_2$]. The direction of current flow is same as that of operation in continuous conduction mode. Similarly, the Equations (25) and (26) of CCM mode exists. The operation of mode 2 terminates whenever the inductor current at time t_2 falls to zero.

*Mode 3: [$t_2 - t_3$]*At this instance all diodes and switches are in OFF state and the voltage at output is maintained with C_0.The equivalent circuit topology corresponding to this mode is illustrated in Figure 5(c). Mode 3 terminates when the switches are at ON state at time t_3 , which is the beginning of subsequent switching period.

E. Modelling of IEEE 13 Bus System

This suggested work makes use of IEEE 13 bus distribution system, which runs at 4.16 kV, has asymmetrical loading, is quite short, and is heavily loaded. In addition, this circuit has a single in-line transformer, overhead and underground wires, shunt capacitors, and a single voltage regulator at the substation. In Figure 6, the proposed topology is illustrated. There are buses with 1, 2, and 3 phases in this IEEE 11 bus system. It has 32 nodes in total. It is expected that each of the 32-circuit nodes has a metre that measures the voltage magnitude. As a result of the closed switch connecting buses 671 and 692, the voltage magnitude of their phases is the same. The load time profiles are the same for all of the loads.

Load Model:

The 13-bus test feeder is a significantly loaded system made up of 3ϕ and 1ϕ loads coupled in delta or Y topology with constant PQ, I, or Z.
Simulink's dynamic load block is used to represent 3ϕ balanced loads, while 1ϕ dynamic load blocks are used to describe the unbalanced loads. Given equations (29) and (30) are the actual power P and reactive power Q for load.

$$P = P_0 \left(\frac{V}{V_0} \right)^{np} \quad (29)$$

$$Q = Q_0 \left(\frac{V}{V_0} \right)^{nq} \quad (30)$$

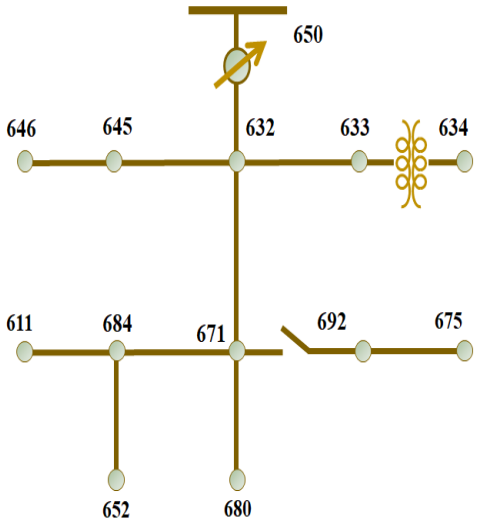

Fig. 6. Configuration of IEEE-13 bus system.

Here, the initial values of voltages, active and reactive power is indicated by V_0, P_0 and Q_0. The constants np and nq regulate the load's PQ, I, or Z type.

RESULTS AND DISCUSSION

The proposed approach consisting of PV, WECS along with battery for steady power studied in this work. The adoption of Switched Z-source boost converter along with PI controller results in stabilized PV voltage. The performance of proposed work based on IEEE 13 bus distribution system is analyzed using MATLAB simulation and the validated results obtained are as follows. Table 1 specifies the parameter specification of Solar, Wind and Battery

.

Table 1:

Spécifications of solar PV system, WECS and BESS

Parameters	Specifications
Solar PV panel	
Peak Power	10kw
No. of Solar PV Panels	750w, 13panels
Short Circuit Voltage	12v
Open Circuit Current	22.6 A
Short Circuit Voltage	62.5A
No. of Series Connected Solar Cells	36
WECS	
No. of Wind Turbines	1
Power	10kw
Voltage	575v
Speed Range	4m/s-16m/s
Switched Z-Source boost converter	
Cz_1,Cz_2	22 μ F
C_0,C_1	1000 μ F
L_1,L_2	4mH
Battery converter	
L	1mH
C	1000 μ F
Switching Frequency	10KHZ
Load	
Capacity	5KW

The waveforms obtained from MATLAB Simulink for the proposed approach are as follows:

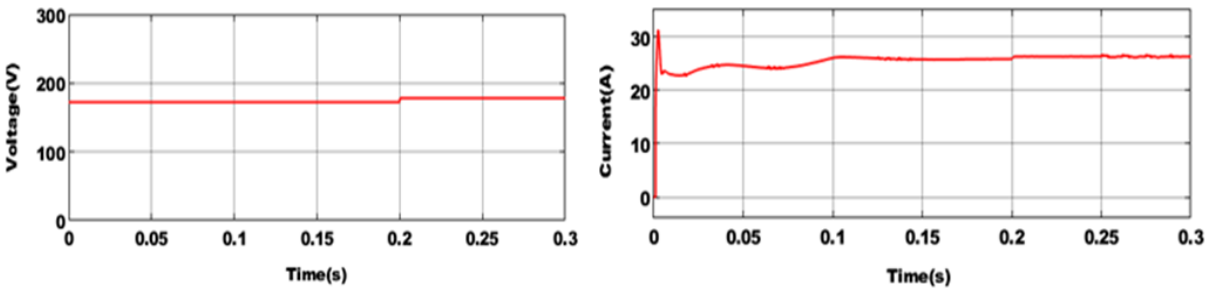

(a) (b)

Fig.7.Solar panel output of (a) voltage and (b) current.

In Figure 7,It is observed that, the input voltage of solar PV is maintained constant after 0.2S while the output current 25A is obtained constant after 0.1s.Corresponding to solar PV outputs at variable operating conditions cause's changes in the converter output.

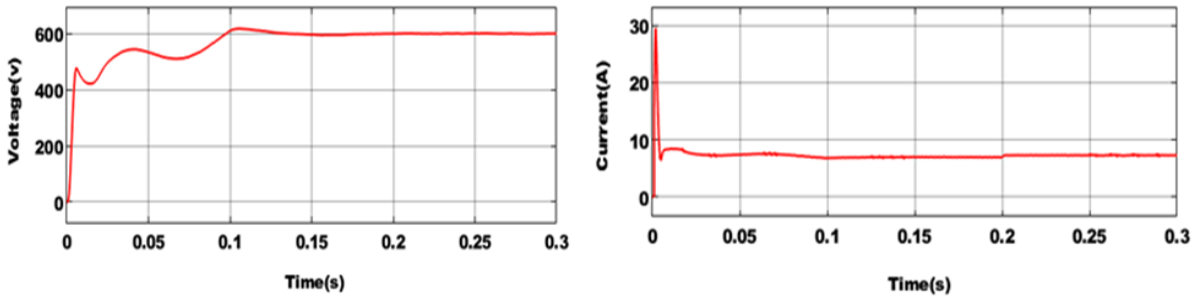

(a) (b)

Fig. 8. Switched Z-Source converter (a) output voltage and (b) output current.

In Figure 8, It is noticed that, the output voltage of converter initially increases with respect to times and fluctuates till 0.1s.A constant voltage of 600V is obtained after 0.1S with the aid of conventional PI controller employed. Similarly, the output current reaches a peak value of 30A and maintained constant after 0.15S with 8A current. Thus the proposed controller approach results in generating improved voltage and current.

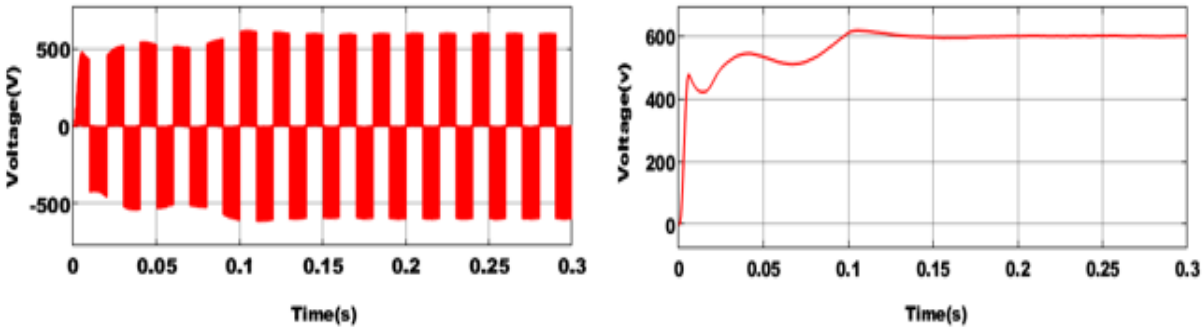

(a) (b)

Fig 9. Output voltage waveform for (a) DFIG –WECS and (b) PWM rectifier.

Owing to to intermittent nature of wind system a constant voltage of 550V is obtained after 0.1S is depicted in Figure 9 (a). Subsequently, after a sudden rise in voltage at 0.02S the converted DC voltage using PWM rectifier achieves a maximum voltage of 600V at 0.1S and is further maintained constant as shown in Figure 9(b).

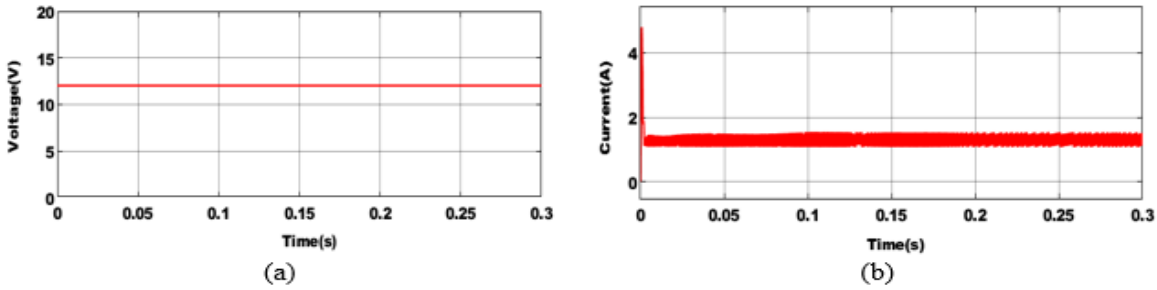

Fig. 10. Battery (a) voltage and (b) current waveform.

Figure 10 represents voltage waveform and current waveform of battery, in which the battery voltage is maintained as a constant of 12V and the corresponding battery current is subjected to minor fluctuations and maintained stable within a short time period.

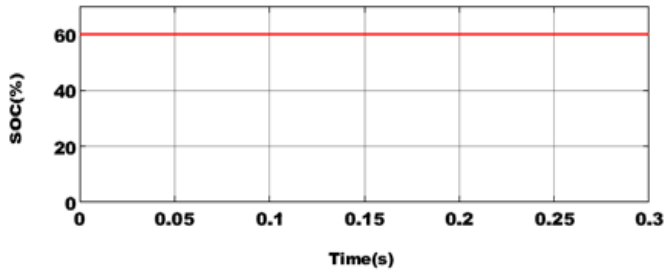

Fig.11. SOC of battery.

The SOC of the bidirectional battery implemented in this work with 60%charge is depicted in Figure 11. Here, the battery operates in buck mode when it is below 60%.At that instance the battery starts charging. While boost operation is performed, when the SOC of battery is above 60%, during this occasion the battery discharges.

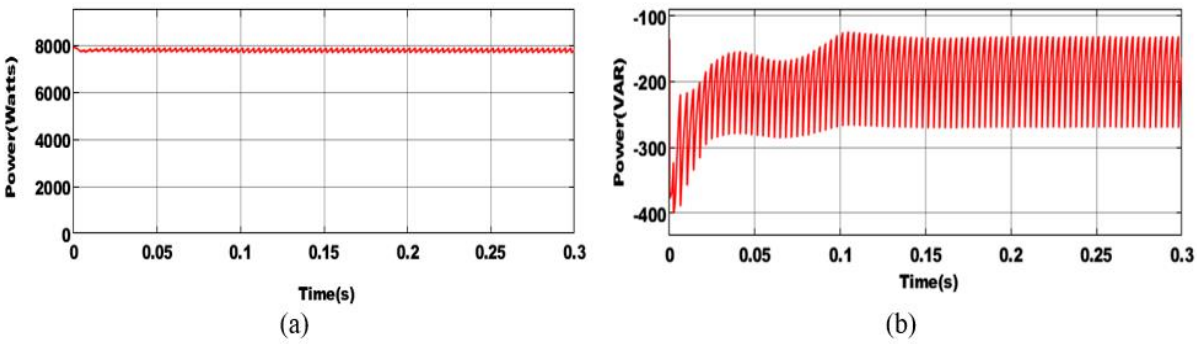

Fig. 12. (a) Real and (b) reactive power waveforms.

The implementation of 13 bus distribution system results in maintaining a constant real and reactive power is illustrated in Figure 12. From figure 12(a), it is observed that a stable real power of 7900W is obtained at 0.03S. Similarly, the corresponding reactive power of -150VARis attained after minor fluctuations as shown in Figure 12(b).

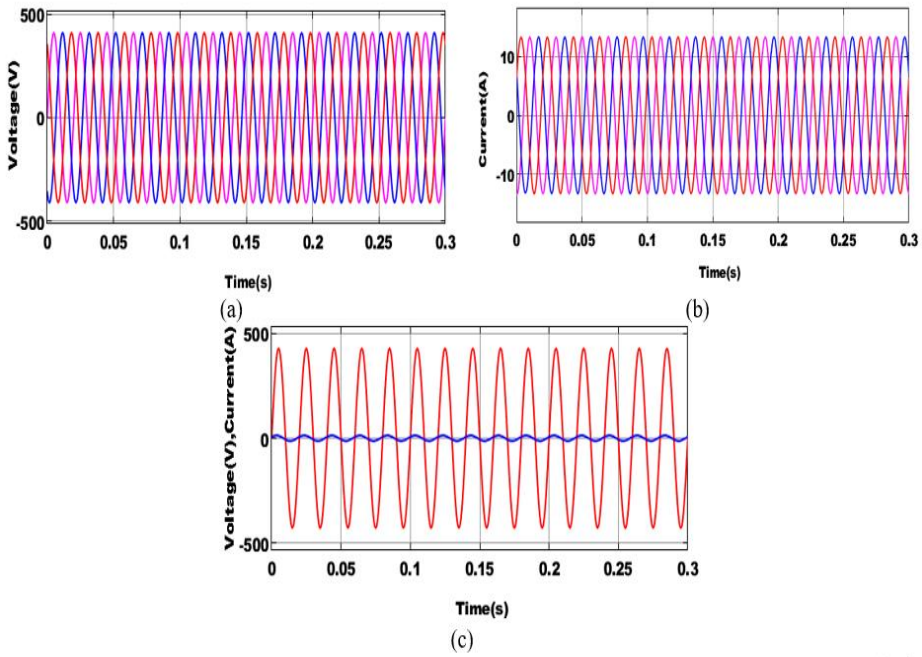

Fig. 13. Waveforms for (a) grid voltage (b) grid current and (c) grid voltage and current.

The waveform illustrated in Figure 13(a) indicates the Grid voltage without any fluctuations. Similarly fromFigure13(b)a stable grid current of 12A is Maintained. A combined waveform for grid voltage and current is depicted in Figure 13(c), in which a stable grid voltage of 450V and Grid current of 12A is maintained.

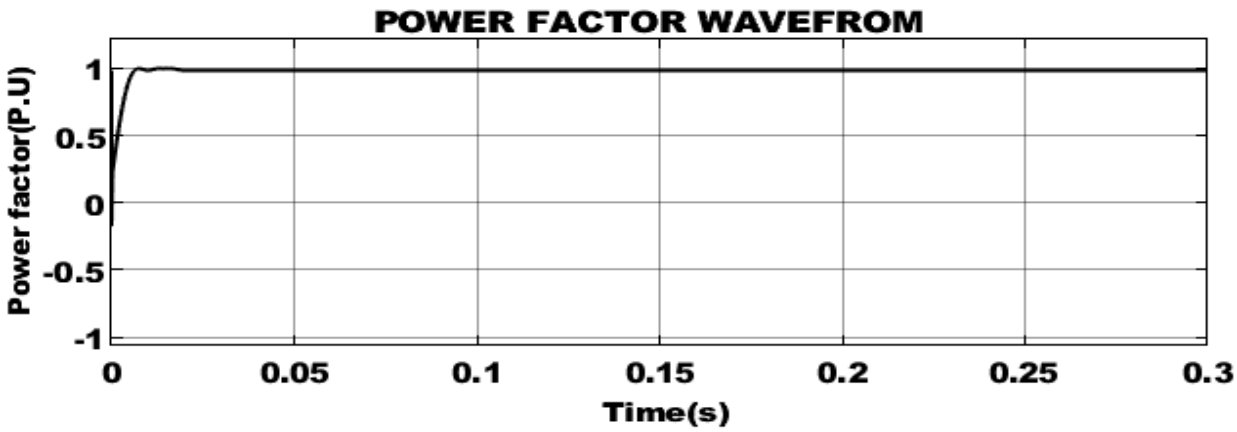

Fig.14. Power factor waveform.

The power factor waveform for the proposed approach is illustrated in Figure 14. From the figure it is observed that, after 0.02s unity power factor is achieved

.

Table 2:
Comparison of Proposed Converter with Existing System.

No. of Diodes	No. of Switches	No. of Inductors	No. of Capacitors	Voltage Gain	Efficiency (%)
4	*2*	*2*	*4*	$G=\frac{1-3D}{1-4D}$	*96.8%*
3	*1*	*3*	*5*	$G=\frac{1}{1-3D}$	*95.6%*
4	*1*	*4*	*7*	$G=\frac{1}{1-4D}$	*95%*
5	*1*	*3*	*7*	$G=\frac{2+D}{1-2D}$	*94.7%*
6	*2*	*2*	*2*	$G=\frac{1+D}{1-3D}$	*94%*

The comparison is performed with existing converters in terms of No. of components, efficiency and voltage gain. The voltage gain comparison is carried out in graph format

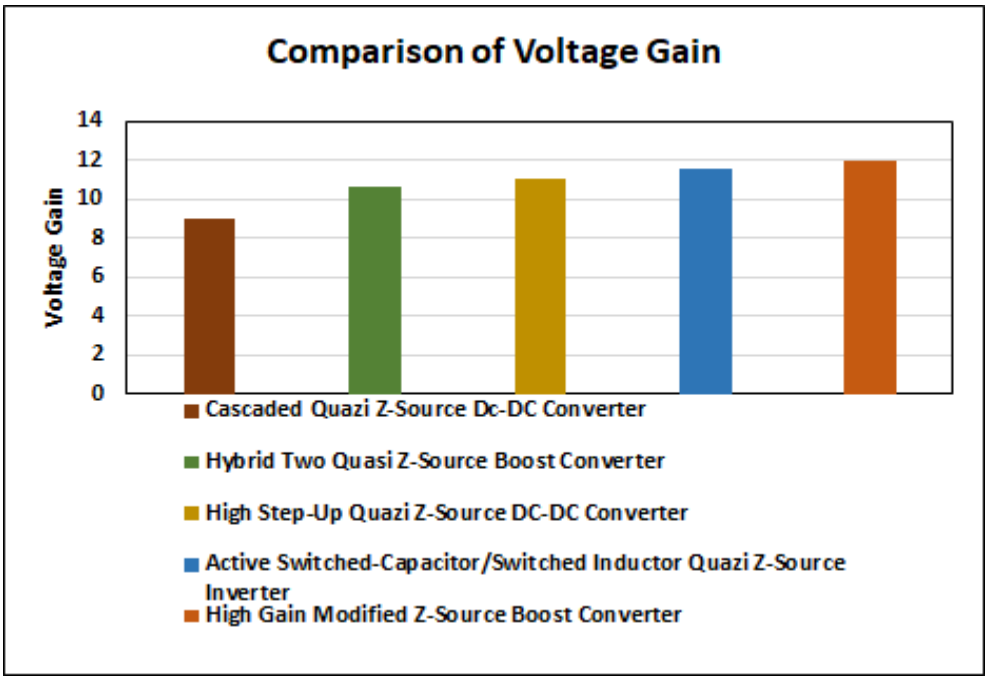

Fig.15.Comparison of voltage gain.

From Figure 15, it is noticed that the proposed High Gain Modified Z-source converter is compared with existing converters, in which the proposed converter attains a voltage gain of 1:12 resulting in higher conversion rang.

CONCLUSION

As the world's energy needs are increasing and conventional energy sources are

running out, and much attention is becoming paid to renewable energy sources. This is because of the sharp rise in energy costs. In this work, HRES combining PV and WECS system is implemented. This study makes a suggestion for an improved DC-DC converter that is completely suited for photovoltaic applications that demand a high level of efficiency. The enhanced DC-DC converter is based on the integration of Z-Source and Boost converters. The utilization of MPSO-PI controller aids is providing stabilized voltage to the converter with better dynamic response. The implemented 13 bus distribution network is simulated with Three Phase system and the corresponding results are obtained using MATLAB Simulink. The comparative analysis is made among different converters in terms of efficiency, in which the proposed Switched Z-Source Boost converter achieves an improved efficiency of 96.8% with reduced harmonics of 0.93% and voltage gain of 1:12 respectively.

References

[1] Kavin K.S., Karuvelam P. Subha. “PV-based grid interactive PMBLDC electric vehicle with high gain interleaved DC-DC SEPIC Converter”, *IETE Journal of Research*, 2021, pp.1-15, doi:10.1080/03772063.2021.1958070.

[2] Bonthagorla P. K., Mikkili S. "Performance Investigation of Hybrid and Conventional PV Array Configurations for Grid-connected/Standalone PV Systems," in *CSEE Journal of Power and Energy Systems*, 2022, vol. 8, no. 3, pp. 682-695, doi: 10.17775/CSEEJPES.2020.02510.

[3] Mosaad M. I., Ramadan H. S. M., Aljohani M. M., El-Naggar F., Ghoneim S. S. M. "Near-Optimal PI Controllers of STATCOM for Efficient Hybrid Renewable Power System," in *IEEE Access*, 2021, vol. 9, pp. 34119-34130, doi: 10.1109/ACCESS.2021.3058081.

[4] Shi Z., Wang W., Huang Y., Li P., Dong L. "Simultaneous optimization of renewable energy and energy storage capacity with the hierarchical control," in *CSEE Journal of Power and Energy Systems*, 2022, vol. 8, no. 1, pp. 95-104, doi: 10.17775/CSEEJPES.2019.01470.

[5] Blaabjerg F., Yang Y., Yang D., and Wang X. "Distributed Power-Generation Systems and Protection," in *Proceedings of the IEEE*, 2017, vol. 105, no. 7, pp. 1311-1331, doi: 10.1109/JPROC.2017.2696878.

[6] Prema V., Bhaskar M. S., Almakhles D., Gowtham N., Rao K. U. "Critical Review of Data, Models and Performance Metrics for Wind and Solar Power Forecast," *in IEEE Access*, 2022, vol. 10, pp. 667-688, doi: 10.1109/ACCESS.2021.3137419.

[7] Wang Z. et al., "Study on the Optimal Configuration of a Wind-Solar-Battery-Fuel Cell System Based on a Regional Power Supply," in *IEEE Access*, 2021, vol. 9, pp.47056-47068, doi: 10.1109/ACCESS.2021.3064888.

[8] Elkay am M., A. Kuperman, "Optimized Design of Multi resonant AC Current Regulators for Single-Phase Grid-Connected Photovoltaic Inverters," in *IEEE Journal of Photovoltaics*, 2019, vol. 9, no. 6, pp. 1815-1818, doi: 10.1109/JPHOTOV.2019.2937386.

[9] Velpula S., Thirumalaivasan R., Janaki M. "Stability Analysis on Torsional Interactions of Turbine-Generator Connected With DFIG-WECS Using Admittance Model," *in IEEE Transactions on Power Systems*, 2020, vol. 35, no. 6, pp. 4745-4755, doi: 10.1109/TPWRS.2020.2992111.

[10] Zhao J., and Chen D."Switched-Capacitor High Voltage Gain Z-Source Converter with Common Ground and Reduced Passive Component," in *IEEE Access*, 2021, vol. 9, pp. 21395-21407, doi: 10.1109/ACCESS.2021.

[11] Nathan K., Ghosh S., Siwakoti Y., Long T, “A New DC-DC Converter for Photovoltaic Systems: Coupled-Inductors Combined Cuk-SEPIC Converter," in *IEEE Transactions on Energy Conversion*, 2019, vol. 34, no. 1, pp. 191-201, doi: 10.1109/TEC.2018.2876454

[12] Errouissi R., Al-Durra A., Muyeen S. M., "A Robust Continuous-Time MPC of a DC–DC Boost Converter Interfaced With a Grid-Connected Photovoltaic System," in *IEEE Journal of Photovoltaics*,2016, vol. 6, no. 6, pp. 1619-1629, doi: 10.1109/JPHOTOV.2016.2598271.

[13] Siouane S., Jovanović S., Poure P."Open-Switch Fault-Tolerant Operation of a Two-Stage Buck/Buck–Boost Converter with Redundant Synchronous Switch for PV Systems," in *IEEE Transactions on Industrial Electronics*, 2019, vol. 66, no. 5, pp. 3938-3947, doi: 10.1109/TIE.2018.2847653.

[14] de Morais J. C. d. S., Morais J. L. d. S. de., Gules R. "Photovoltaic AC Module Based on a Cuk Converter with a Switched-Inductor Structure," in *IEEE Transactions on Industrial Electronics*, 2019, vol. 66, no. 5, pp. 3881-3890, doi: 10.1109/TIE.2018.2856202.

[15] Liu J., Wu J., Qiu J., Zeng J. "Switched Z-Source/Quasi-Z-Source DC-DC Converters With Reduced Passive Components for Photovoltaic Systems," in *IEEE Access*, 2019, vol. 7, pp. 40893-40903, doi: 10.1109/ACCESS.2019.2907300.

[16] Ahmed, K. Y., Bin Yahaya N. Z., Asirvadam V. S., Saad N., Kannan R., Ibrahim O. "Development of Power Electronic Distribution Transformer Based on Adaptive PI Controller," in *IEEE Access*, 2018, vol. 6, pp. 44970-44980, doi: 10.1109/ACCESS.2018.2861420.

[17] Alshareef M., Lin Z., Li F., Wang F. "A grid interface current control strategy for DC microgrids," in *CES Transactions on Electrical Machines and Systems*,2021, vol. 5, no. 3, pp. 249-256, doi:10.30941/CESTEMS.2021.00028.

[18] Imtiaz B., Zafar I., and Yuanhui C. "Modelling of an Optimized Micro grid Model by Integrating DG Distributed Generation Sources to IEEE 13 Bus System", *European Journal of Electrical Engineering and Computer Science*, 2021, vol.5, no.2, pp.18-25, doi;10.24018/ejece.2021.5.2.309.

[19] Farrokhabadi M., König S., Cañizares C. A., Bhattacharya K., Leibfried T. "Battery Energy Storage System Models for Micro grid Stability Analysis and Dynamic Simulation," 2018, in *IEEE Transactions on Power Systems*, vol. 33, no. 2, pp. 2301-2312, doi: 10.1109/TPWRS.2017.2740163.

[20] Mahela O. P., Khan B., Alhelou H. H., P. Siano. "Power Quality Assessment and Event Detection in Distribution Network With Wind Energy Penetration Using Stock well Transform and Fuzzy Clustering," in *IEEE Transactions on Industrial Informatics*, 2020, vol. 16, no. 11, pp. 6922-6932, doi: 10.1109/TII.2020.2971709.

[21] Vinnikov D., Roasto I., Strzelecki R., and M. Adamowicz. "Step-Up DC/DC Converters With Cascaded Quasi-Z-Source Network," in *IEEE Transactions on Industrial Electronics*, 2012, vol. 59, no. 10, pp. 3727-3736, doi: 10.1109/TIE.2011.2178211.

[22] Shen H., Zhang B., and Qiu D., "Hybrid Z-Source Boost DC–DC Converters," in *IEEE Transactions on Industrial Electronics*, 2017, vol. 64, no. 1, pp. 310-319, doi: 10.1109/TIE.2016.2607688.

[23] Haji-Esmaeili M. M., Babaei E., and M. Sabahi. "High Step-Up Quasi-Z Source DC–DC Converter," in *IEEE Transactions on Power Electronics*, 2018, vol. 33, no. 12, pp. 10563-10571, doi: 10.1109/TPEL.2018.2810884

Information about authors.

Sathish Ch.,
Research Scholar,
Department of Electrical and Electronics Engineering,
Annamalai University,
Tamil Nādu, India,
The field of Scientific Interest is the power system,
Email:
anusmin2@gmail.com

Manikandan M.,
Ph.D., Professor,
Department of Electrical and Electronics Engineering,
Jyothismathi Institute of Technology and science,
Telangana, India, Field of scientific interest is Power Quality in Electrical Distribution systems,
Email:
cm.manikandan@gmail.com

Chidambaram I.A.,
Ph.D., Professor,
Department of Electrical and Electronics Engineering,
Annamalai University,
Tamil Nādu, India, Field of scientific interest is Power Quality in Electrical Distribution systems.
Email:
driacdm@gmail.com